cosmetics

MDPI

*Article*

# Impact of Fatty Acid Composition of Polyglycerol Esters on the Emulsifying Performance in Cosmetic Formulations

**Julie Rossero *, Maxime Nollet, Nicolas Ritter and Jean-David Rodier**

Department of Research and Development, Gattefossé SAS, 36 Chemin de Genas, 69804 Saint-Priest, France; mnollet@gattefosse.com (M.N.); nritter@gattefosse.com (N.R.); jrodier@gattefosse.com (J.-D.R.)
* Correspondence: jrossero@gattefosse.com

**Abstract**

The cosmetics industry continually seeks innovations that deliver ever-higher performance while meeting growing sustainability requirements. Although numerous plant-derived surfactants have recently emerged, achieving performance levels comparable to synthetic benchmarks remains challenging. In this study, we aimed to design a natural polyglycerol-10 ester (PG-10 ester) capable of stabilizing demanding systems such as high-internal-phase nano-emulsions (nano-HIPE) and mineral oil-in-water sunscreens. We investigated the key parameters governing surfactant efficiency: fatty acid composition from C12 to C22 or their blends, the presence of partial glycerides, and reaction parameters. Various polyglycerol esters were synthesized and characterized through chromatographic analysis and HLB determination, and then incorporated into formulations to assess their performance. This work made it possible to identify four parameters as essential for achieving high surfactant efficiency: (i) grafting multiple fatty acids onto a single polyglycerol backbone, (ii) combining short/medium-chain (<C16) and long-chain (≥C16) fatty acids, (iii) including partial glycerides within the surfactant, and (iv) allowing the reaction medium to reach full equilibrium. Achieving full equilibrium results in synthesis medium clarity, which allows the HLB value to rise from 6 to 7 to 11–12 and ensures complex emulsion stability. This rational design approach led to a natural PG-10 ester whose performance equals that of conventional synthetic benchmarks, providing a significant advancement toward sustainable high-performance surfactant technologies.

**Keywords:** polyglycerol esters; stability; nano-HIPE; HLB; O/W sunscreen; fatty acid composition; partial glycerides; clarity

Check for updates

Academic Editors: Richard Daniellou and Enzo Berardesca

Received: 8 April 2026
Revised: 7 May 2026
Accepted: 20 May 2026
Published: 22 May 2026

**Copyright:** © 2026 by the authors. Licensee MDPI, Basel, Switzerland. This article is an open access article distributed under the terms and conditions of the Creative Commons Attribution (CC BY) license.

## 1. Introduction

Over the past decade, the cosmetics industry has faced increasing pressure to deliver safer, more transparent, and more environmentally responsible products [1,2]. This shift toward "responsible and renewable" cosmetics requires rethinking raw materials, manufacturing processes, and evaluation methods in order to replace controversial ingredients, reduce environmental impact, and promote bio-sourced alternatives to synthetic compounds [3,4]. Balancing performance, safety, and sustainability while preserving sensory experience and effectiveness is a central challenge for the industry. Within this context, the present work aims to develop a highly efficient, 100% bio-sourced non-ionic surfactant capable of stabilizing complex emulsions that are particularly demanding in terms of feasibility and long-term stability.

Although numerous natural surfactants have already been developed, achieving performance levels comparable to synthetic surfactants remains particularly challenging [5]. Developing natural ingredients that match the efficiency, robustness, and versatility of their synthetic counterparts continues to be a major hurdle in advancing fully bio-based formulations. Formulations such as transparent high-internal-phase nano-emulsions (nano-HIPE) or oil-in-water (O/W) sunscreens containing a high concentration of mineral filters clearly illustrate this point.

Indeed, O/W nano-HIPEs are highly attractive cosmetic systems due to their numerous functional advantages. These systems have been known for decades, yet they continue to attract significant research interest because they remain difficult to manufacture and stabilize [6]. These concentrated emulsions—used as makeup removers, exfoliants, or massage oils—combine transparency, easy rinsability without leaving an oily residue, and the ability to form transparent gel-like emulsions of a few hundred nanometers using a minimal amount of surfactant [7]. Their formulation does not require strict HLB adjustment [8], but their implementation remains technically demanding, which explains the strong research interest in these systems [9]. These colloidal systems appear as gels and are classified as oil-in-water (O/W) or oil-in-detergent (O/D) [10] emulsions containing a high internal oil phase (>74%) [6,7,9,11,12]. Nano-HIPEs are composed of only four components (surfactant, oil, water and polyol) and their gel zone is consistently located in the same region of the ternary diagram, as shown in Figure 1.

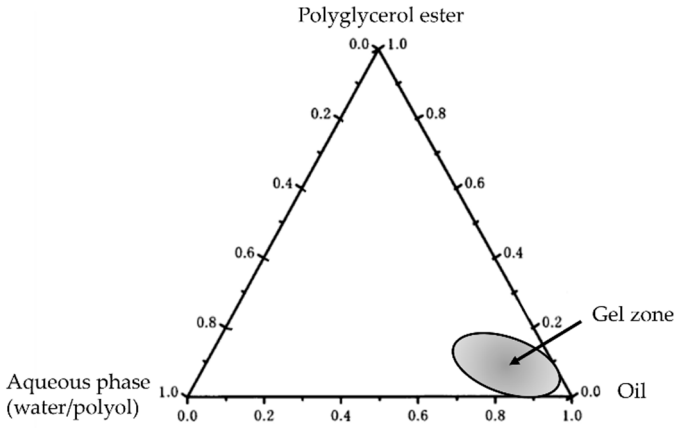



**Figure 1.** Gel region localization within the a surfactant/aqueous phase/oil system ternary phase diagram [13].

Currently, the surfactants used to formulate these types of systems are primarily petrochemical-derived, like ethoxylated surfactants or sucroesters [7,14]. Although sucroesters are of natural origin, their synthesis requires toxic organic solvents (e.g., DMSO, DMF) [15,16], and their use in formulation is delicate. Formulating these nano-HIPEs with sucrose esters is particularly challenging, as they require long hydration times and the oil phase must be added dropwise to avoid destabilization.

Direct O/W sunscreens containing mineral UV filters are also gaining interest in the cosmetics industry. This trend is driven by concerns surrounding organic filters, which are often associated with endocrine-disrupting effects and significant aquatic toxicity [17,18]. As a result, mineral filters such as titanium dioxide and zinc oxide have emerged as safer alternatives [19]. However, achieving high sun protection factor (SPF) values with mineral filters requires substantial concentrations, making their incorporation into O/W emulsions difficult. Indeed, these filters are typically coated with lipophilic materials to improve dispersion in the oil phase, which inherently favors W/O systems. Consequently,

developing stable, effective, and sensorially pleasant O/W sunscreens containing high levels of mineral filters remains a key formulation challenge.

Non-ionic surfactants commonly used in cosmetics fall into three main groups: polyethylene glycol (PEG)-based surfactants, glycerol-based surfactants and sugar-based surfactants. PEG derivatives are widely employed due to their high efficiency and low irritancy, but they are petroleum-derived, and their synthesis can generate by-products such as 1,4-dioxane, a classified carcinogen [20]. Glycerol-based surfactants include simple glycerol esters, typically suited for W/O emulsions because of their low HLB [21], as well as polyglycerol derivatives whose HLB can be tuned by adjusting oligomer length. Using large polyglycerol oligomers such as commercial polyglycerol-10 (PG10) with relatively short aliphatic chains allows the production of esters with HLB values up to 15–16, enabling their use as surfactants, solubilizers, humectants, or dispersing agents across diverse formulations [22–24]. Their properties can therefore be tailored to the intended application. Moreover, polyglycerol esters are synthesized from 100% naturally derived raw materials through a simple, solvent-free process that generates no harmful by-products [25].

The present study identified the key parameters required to synthesize a polyglycerol ester capable of forming and stabilizing complex emulsions such as nano-HIPEs and mineral O/W sunscreens. The work focuses on the influence of the fatty acid composition of PG10 esters on their stabilizing properties. To this end, various polyglycerol-10 fatty-acid esters were synthesized, characterized, and incorporated into nano-HIPEs and mineral O/W sunscreen formulations. PGFE characterization was carried out through HLB determination using the PIT-slope method [26] and UHPLC-CAD analysis. Emulsion stability was evaluated through accelerated stability tests, including storage for 1 month at 50 °C, 3 months at 40 °C, and three successive freeze–thaw cycles, in order to simulate demanding storage or transport conditions.

## 2. Materials and Methods

### *2.1. Synthesis and Formulation Materials*

For the synthesis of various polyglycerol fatty acid esters, vegetable polyglycerin-10 (PG10) was sourced from SPIGA Nord S.p.A., Italy (hydroxyl value 800–850 mg KOH/g). Hydrogenated palm kernel oil (HPKO), hydrogenated palm oil (HPO) and hydrogenated coprah oil (HCO) were obtained from ADM-SIO. Cuphea oil was provided by the USDA ARS National Center for Agricultural Utilization Research in Peoria, Illinois and Hermetica Illucens oil (Hilucia$^{TM}$) oil for Monogastrics from Inovafeed. C16/C18 fatty acids (stearin) was sourced from Cremer, and caprylic/capric triglycerides (MCT) were supplied by Gattefossé SAS. The fatty acids from C8 to C18 for analysis were provided by Sigma.

For the preparation of transparent nano-HIPE, glycerin was obtained from SPIGA Nord (Caronno Pertusella, Italy) and the water used was deionized. For sunscreen emulsions, zinc dispersion was sourced from Antaria Ltd (Malaga, WA, Australia), cococaprylate from BASF (Ludwigshafen, Germany), Kelco Care diutan gum from Lubrizol Corporation (Wickliffe, OH, USA) and cetearyl alcohol and phenoxyethanol (and) ethylhexylglycerin were obtained from KOBO Products Inc. (South Plainfield, NJ, USA).

### *2.2. Synthesis of Polyglycerol-10 Fatty Acid Esters*

Various polyglycerol-10 fatty acid esters were synthesized through esterification and/or alcoholysis/transesterification reactions following standard procedures [27]. Vegetable polyglycerine-10 (SPIGA Nord S.p.A) was reacted with fatty acids and/or triglyceride oils. The molar ratio between PG10 and fatty acids used is identical for all prototypes: 1 molar equivalent of PG10 for 2 molar equivalents of fatty acids regardless of whether the fatty acid source was a triglyceride oil or free fatty acids. The reaction was carried out

under nitrogen gas in the presence of a basic catalyst at a high temperature. The reaction was terminated when the acid value dropped below 1 mg KOH/g, and/or solid-phase extraction analyses confirmed no further changes in triglyceride (TG) composition when oil was used. The product was then neutralized with orthophosphoric acid to remove soaps, decanted if necessary, and hot-filtered.

#### 2.2.1. Determination of Hydrophilic-Lipophilic Balance (HLB)

The Hydrophilic–Lipophilic Balance (HLB) value, introduced by Griffin [28], can be calculated or measured using the PIT-slope method (Phase Inversion Temperature) [26,29] like in this work. This method is based on the phase inversion temperature deviation (PITd) of the CiEj/n-octane/water emulsion system. The PITd of a substance under investigation is the slope of the equation describing the variation in the phase inversion temperature between the water/octane/C10E4 system and the system with the addition of the studied substance. The measurement was performed with a Radiometer Analytical CDM 210 conductivity meter equipped with a probe that simultaneously records conductivity and temperature.

First, the reference solution C10E4/n-octane/brine with 3% surfactant was prepared in a 20 mL vial and placed in a thermostated cell connected to a cryothermostat (Ministat-230-NR, Huber GmbH, Offenburg, Germany). A heating cycle at 1 °C/min was performed under magnetic stirring, and the conductivity profile as a function of temperature was obtained. Then, the surfactant to be tested was introduced into the system by successive additions, and a heating cycle was applied each time to determine the PIT value. The PIT-slope was then determined using a relation linking the mass fraction of the added test surfactant to the phase inversion temperature deviation. Finally, the HLB was calculated using the correlation curve between HLB and PIT established for this system, as described in the article [26]:

$$\mathrm{PITd} = 2.1\mathrm{HLB} - 25.4 \quad (1)$$

#### 2.2.2. Polyglycerol-10 Oligomers Distribution

Because the polyglycerol-10 used for ester synthesis is a mixture of oligomers of different polymerization degrees, its composition was analyzed by ultra-high-performance liquid chromatography coupled with a charged aerosol detector and mass spectrometry (UHPLC-CAD-MS). Chromatographic analyses were performed using a Bruker HPLC–MS system controlled by HyStar. Samples were dissolved in acetonitrile/water under ultrasound and vortexing until clear. Separation was achieved using a Cogent Diamond Hybride 150 × 4.6 mm, 4 µm column at 35 °C with CAD at 40 °C, and a gradient of acetonitrile/water with a flow rate of 0.8 mL.min$^{-1}$. The eluent was split between the MS and CAD. Mass spectra were acquired in positive mode, and EICs were extracted for sodium-adducted oligomers from PG2 to PG11 ($m/z$ 189–855) and their dehydrated forms ($m/z$ 171–837). This analytical procedure is an internal method and the oligomer distributions reported here correspond to relative percentages. Absolute quantification was not possible, as no certified analytical standards are available for these polyglycerol oligomers.

#### 2.2.3. Determination of the Ester Composition by Chromatographic Analysis

The composition of polyglycerol-10 esters was determined by chromatographic analysis using an internal method. The quantity of free polyglycerol-10 and its oligomer distribution were analyzed by ultra-high-performance liquid chromatography coupled with a charged aerosol detector Dionex UltiMate 3000 UHPLC (Thermo Fisher Scientific Inc., Waltham, MA USA) (UHPLC-CAD) using a Phenomenex AerisWidePore-XBC8 column (Phenomenex Inc., Torrance, CA, USA) and a gradient of water/MeOH, then MeOH and finally IsopOH/THF. The relative proportions of monoesters, diesters, and triesters in each

prototype were analyzed by UHPLC coupled with amazon speed ETD mass spectrometer (Bruker Daltonics GmbH & Co. KG, Bremen, Germany) (MS), using the same column and solvent gradient. An initial identification of the species was carried out by determining the major ions present at each time. Then, using the theoretical masses listed, an inventory of the ions detected by mass and by sample was carried out. Finally, a specific extraction of the masses was performed on the esterified majority oligomers in relation to the initial distribution of polyglycerol oligomers. This made it possible to obtain a distribution in relative percentages of the different types of esters.

#### 2.2.4. Melting Range Measurement

The melting range of some polyglycerol-10 esters was determined by power-compensated differential scanning calorimetry (DSC), which allows the phase transitions of a sample to be highlighted [30]. The differences in heat exchange between the sample to be analyzed and a reference (an empty capsule) were measured, allowing the various changes in state to be observed. The product underwent a temperature increase from −20 °C to 120 °C at a heating rate of 3.00 °C/min. It then underwent a temperature decrease from 120 °C to −20 °C, followed by a second temperature increase from −20 °C to 120 °C. These two temperature increases were performed during the program: first, to clear the product's thermal history, and second, to take the usable measurement.

### *2.3. Mineral Sunscreen Emulsions Preparation*

Sunscreen emulsions containing a large amount of mineral UV filters (zinc oxide dispersion) were prepared. 0.15 wt% of Kelco-CareTM Diutan Gum was dispersed in 50.05 wt% of water and mixed for 5 min using a deflocculator. Then, 2 wt% of glycerin was added and the pH of the aqueous phase was adjusted between 5.5 and 6.5 with citric acid. Meanwhile, the oil phase was prepared by weighting 38 wt% of zinc dispersion (Zinclear® XP65 Coco), 3 wt% of coco-caprylate oil, 0.5 wt% of cetearyl alcohol, 0.7 wt% of a preservative (PE 9010) and 4 wt% of the surfactant to be tested. The emulsion was prepared at 65 °C using a stirrer VMI Rayneri (Montaigu-Vendée, France) and then cooled using a water bath.

### *2.4. Preparation of Transparent Nano-HIPE Stabilized by Polyglycerol-10 Esters*

According to the literature [13,31–33], the nano-HIPEs formulations correspond to the gel zone of the surfactant/aqueous phase/oil system. This area is always located in the same space in the ternary diagram regardless of the raw materials used: it is a zone very rich in oil with a low surfactant concentration (Figure 1). 3 wt% of PG10 fatty acid esters was mixed with 83 wt% caprylic/capric triglycerides (MCT) at 60 °C until the surfactant was fully solubilized. Separately, 5 wt% of water was combined with 9 wt% of glycerin and heated at 60 °C. The nano-HIPE was prepared by mechanical shearing at 550 rpm using a Turbotest VMI with a propeller at high 60 °C. The oily phase was added dropwise at 60 °C to the aqueous phase until a clear gel emulsion was obtained.

### *2.5. Nano-HIPEs and Sunscreens Stability: Accelerated Stability Tests*

The stability of the transparent nano-HIPE and the sunscreens was assessed at various temperatures to ensure that the formulations met the intended physical and chemical quality standards [34]. Glass pillboxes containing 30 mL of the different emulsion samples were stored at room temperature for six months, at 40 °C for three months, and at 50 °C for one month. The formulation stability is assessed through visual inspection or their appearance (odor, color, texture) and the absence of instability phenomena such as sedimentation, creaming, or phase separation. Additionally, freeze–thaw tests were carried out on the various formulations to assess their resistance to extreme transport and storage conditions. The

nano-HIPEs and sunscreens underwent 3 freeze/thaw cycles with temperatures ranging from −24 °C to room temperature. A formula must pass all these tests to be considered stable and suitable for application.

## 3. Results

### *3.1. Influence of Fatty Acid Composition of Polyglycerol-10 Esters on the Stability of Nano-HIPE*

#### 3.1.1. Polyglycerol-10 Esters with a Single Fatty Acid: PG10-1FA

First of all, the commercial polyglycerol-10 used in this work was analyzed in order to have more information about molecular composition of synthetized polyglycerol esters. The results obtained by chromatographic analysis are presented in Figure 2. It is important to note that the response coefficients for the various species are not known; therefore, the results shown in this figure are given as relative area percentages. The polyglycerol used in this study exhibits an oligomer distribution centered around PG4 and PG5, with species extending up to PG12. Only partial separation was achieved by CAD due to the broad dispersity of the oligomer mixture. In addition, the commercial polyglycerol-10 sample was found to contain a substantial proportion of oligomers that had lost one, two, or even three water molecules, corresponding to mono-, di-, and tri-cyclized species. In Figure 2, cyclic and linear oligomers are grouped in the same category.

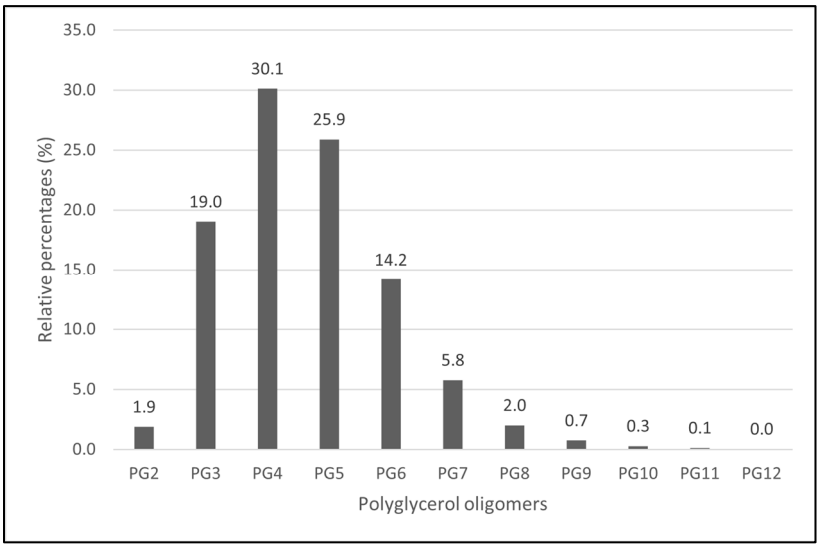



**Figure 2.** Oligomer distribution of commercial Polyglycerol-10 used for esters synthesis.

In conclusion, the polyglycerol-10 used as the starting material for surfactant synthesis exhibits a highly complex structural profile, owing to its broad oligomer distribution and the presence of multiple cyclized species.

Subsequently, polyglycerol-10 esters were synthesized with polyglycerol-10 as the hydrophilic part and a saturated linear fatty acid as the hydrophobic part. The molar ratio between polyglycerol and the fatty acid was identical across all prototypes, with 1 molar equivalent of polyglycerol-10 for 2 molar equivalents of fatty acids. The FAs selected were those most commonly used in the cosmetics industry, lauric acid (C12), myristic acid (C14), palmitic acid (C16), stearic acid (C18), and behenic acid (C22). Once synthesized, these various esters were characterized, and the results are presented in Table 1.

Based on Table 1, it can be said that the HLB values are logically related to the length of the aliphatic chain [25]. The shorter the fatty acids, the more hydrophilic the resulting esters will be, and therefore the higher their HLB. One prototype is an exception: PG10-C18, which has a lower HLB than PG10-C22 despite having a shorter hydrophobic chain. This can be explained by the relative distribution of the esters. According to the

chromatographic analyses, PG10-C18 consists of 72% monoesters and 28% diesters, whereas PG10-C22 is composed almost exclusively of monoesters. Given that diesters are much more hydrophobic than monoesters, this may explain the difference in HLB. It should be noted that the proportions of monoesters, diesters, and triesters must be interpreted with caution. Because no analytical standards exist for these molecules, the results reflect relative rather than absolute percentages. In addition, the response factors of the different species are unknown, which may introduce further bias.

**Table 1.** Physicochemical characteristics of synthesized polyglycerol-10 fatty acid esters.

| Prototypes | HLB | Melting Range (°C) | Ester (%) | Monoester/ Diesters/Triesters (%) | Free PG10 (%) |
|---|---|---|---|---|---|
| PG10-C12 | 13.0 | 9.49–20.89 | 80 | 78/14/8 | 20 |
| PG10-C14 | 11.5 | 17.92–21.20 | 80 | 51/41/8 | 20 |
| PG10-C16 | 11.0 | 35.34–37.78 | 90 | 57/42/0 | 10 |
| PG10-C18 | 9.0 | 51.28–57.52 | 55 | 72/28/0 | 45 |
| PG10-C22 | 10.0 | 70.78–73.01 | 38 | 97/3/0 | 62 |

Regarding the melting range of the prototypes (Table 1), it logically increases as the length of the aliphatic chain increases. The esters obtained are solid at room temperature for aliphatic chains containing 16 carbons. In this study, temperature ranges associated with thermal transitions were determined rather than precise temperatures because the synthesized polyglycerol esters consist of a mixture of esters (mono-, di-, and triesters) combined with various polyglycerol oligomers (PG4, PG5, PG6, etc.).

On the other hand, we can see that we obtained good yields for aliphatic chains up to 16 carbons. This is because polyglycerol-10 remains soluble and homogeneous in these esters, whereas for larger aliphatic chains, part of the PG10 does not react. The affinity between polyglycerol-10 and C18 or C22 fatty acids appears to be very low. In fact, during the synthesis of polyglycerol esters, fatty acids and polyglycerol-10 are initially insoluble in one another. Mechanical agitation is used to force these molecules to combine and form esters that are soluble in both phases. Depending on the size of the aliphatic chain, the resulting ester will be more or less hydrophilic. The PG10-C18 and PG10-C22 prototypes, which have very large aliphatic chains, are more hydrophobic than the other prototypes; so, the polyglycerol-10 has difficulty solubilizing in these esters resulting in lower yields of esters and a lot of free PG10.

Regarding the relative ester composition of the various prototypes shown in Table 1, we can observe that it varies greatly depending on the chain length of the fatty acids. Indeed, in the reaction medium, two immiscible phases coexist: polyglycerol-10 and the fatty acids. When a short-chain fatty acid (e.g., C12) esterifies PG10 to form a monoester, the resulting species is more soluble in the polyglycerol phase than in the fatty acid phase, which drives the reaction predominantly toward monoester formation. As the alkyl chain length of the fatty acid increases, the monoester becomes more soluble in the fatty acid phase than in polyglycerol-10, making the formation of di- and triesters thermodynamically more favorable, as observed for the PG10-C12, PG10-C14, and PG10-C16 systems. However, the solvent used for ester analysis cannot solubilize highly hydrophobic species, introducing a bias for long-chain di- and triesters ($\geq$C16), whose quantification must therefore be interpreted with caution. For the PG10-C18 and PG10-C22 samples, the composition reported here corresponds only to the fraction soluble in the analytical solvents. This does not imply that these materials do not contain diesters or triesters, but rather that such species are not detected with this method.

Once synthesized and characterized, the various prototypes were tested in formulation. Each ester was tested individually as a single emulsifier to stabilize a nano-HIPE, and the results are presented in Table 2.

**Table 2.** Stability of nano-HIPEs formulated with PG10 ester and one saturated linear acid.

| Prototypes | Nano-HIPE Stability |
|---|---|
| PG10-C12 | X |
| PG10-C14 | X |
| PG10-C16 | Stable at room temperature (RT) but not at heat |
| PG10-C18 | X |
| PG10-C22 | X |

X = No formation of stable nano-HIPE even at RT.

Based on Table 2, we can say that none of the prototypes produced a stable nano-HIPE according to our criteria, even at room temperature. The emulsions broke down during the oil phase incorporation stage or during cooling. Only PG10-C16 produced a stable nano-HIPE at room temperature for several weeks, but it failed when exposed to heat or freeze/thaw cycles.

As previously mentioned, the transparent nano-HIPEs currently available on the market are mainly formulated with sucrose esters. However, it has been noted that these sucrose esters are always used in combination, most often sucrose laurate with sucrose palmitate [35]. Based on this observation, further tests were carried out by combining polyglycerol-10 esters to attempt to formulate nano-HIPEs that meet our stability criteria.

#### 3.1.2. Mixture of Two Different PG10-1FA Esters: PG10-1FA$_A$ + PG10-1FA$_B$

The previously synthesized esters were tested in combinations of two in nano-HIPEs, and the results are presented in Table 3. Only the PG10-C22 prototype was not included in the tests due to its low manufacturing yield (38%), which compromises its economic viability.

**Table 3.** Stability results of nano-HIPEs formulated with binary blends of PG10 fatty acid esters: PG10-1FA$_A$ + PG10-1FA$_B$.

| Combinations | PG10-C12 | PG10-C14 | PG10-C16 | PG10-C18 |
|---|---|---|---|---|
| PG10-C12 | No nano-HIPE | | | |
| PG10-C14 | No nano-HIPE | No nano-HIPE | | |
| PG10-C16 | OK at RT | OK at RT | | |
| PG10-C18 | OK at RT | OK at RT | OK at RT | |
| PG10-C22 | OK at RT | OK at RT | OK at RT | No nano-HIPE |

Based on Table 3, we can conclude that we obtain better results by combining two PG10 esters rather than using them alone. By combining two PG10 esters, it was possible to formulate nano-HIPEs that remained stable at room temperature for several weeks, unlike the prototypes used alone. The combinations that gave the best results were: PG10-C12 + PG10-C16; PG10-C12 + PG10-C18; PG10-C14 + PG10-C16; PG10-C14 + PG10-C18 et PG10-C16 + PG10-C18.

However, these gels remained unstable when exposed to heat and/or freeze/thaw cycles, as shown Figure 3. These instabilities can be explained by the crystalline structure of the polyglycerol esters. Indeed, as the hydrophobic part of the synthesized polyglycerol esters consists of a single type of fatty acid, these fatty acids will organize themselves

into a highly ordered structure forming crystals. Our hypothesis is that the surfactant crystals located at the droplet interface grow large enough to pierce the interfacial film, thereby triggering emulsion destabilization. This phenomenon is described in various articles [36–38] and shown in Figure 4.



**Figure 3.** Photograph of a nano-HIPE after three freeze/thaw cycles formulated with PG10-C16 + PG10-C18.

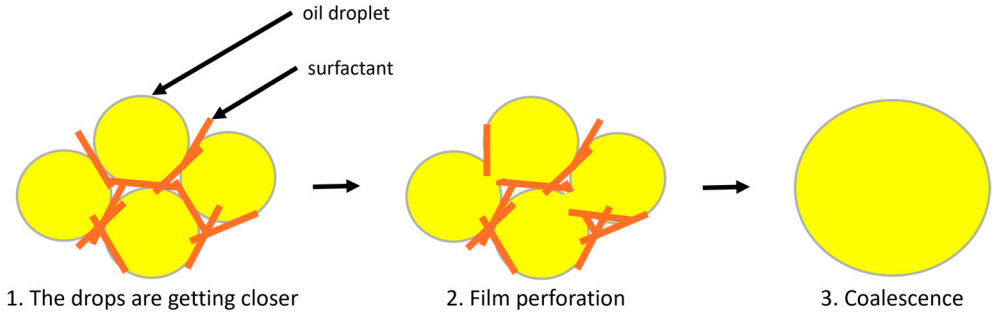



**Figure 4.** Mechanism of destabilization in partially crystallized emulsions.

Indeed, at room temperature, the system was immobilized so the gel remained stable. However, the polyglycerol esters at the interface of the oil droplets formed large crystals that acted like needles. These crystals could pierce the droplets and destabilize the system. Consequently, when the nano-HIPE is frozen, oil leaks occur, causing the structure to break down. Conversely, when the nano-HIPE is heated, the temperature exceeded the melting point of the PG esters, causing the crystals to melt. This led to coalescence and destabilization of the nano-HIPE. This phenomenon is consistent with the results shown in Table 3. Nano-HIPEs exhibit stability at room temperature but not when exposed to heat or during freeze–thaw cycles.

To counteract this effect, the strategy adopted was therefore to introduce disorder into the structure to form smaller crystals [39]. To achieve this, mixtures of fatty acids grafted onto the same polyglycerol were used. In fact, by grafting various fatty acids onto the same polyglycerol, we obtained a much greater diversity of esters than by using two pure polyglycerol esters. This diversity of the esters formed introduced disorder into the surfactant's crystal structure, thereby limiting the formation of large crystals capable of piercing the droplets So, mixture of different free fatty acids and oils containing various fatty acids of variable chain lengths were tested.

#### 3.1.3. Polyglycerol Esters with Various FAs or Oil: PG10-nFA or PG10-Oil

In order to introduce disorder in the nano-HIPE structure, several synthesis were carried out in a "one pot" with oils or mixtures of FAs: one with medium-chain triglycerides (MCT), one with hydrogenated palm kernel oil (HPKO); one with hydrogenated palm oil (HPO); and one with stearin, which is a mixture of free fatty acids (50/50 palmitic acid

and stearic acid). The esters PG10MCT and PG10HPKO are mainly composed of short- and medium-chain fatty acids (<16C), while PG10HPO and PG10C16C18 contain mostly long-chain fatty acids (≥16C). Table 4 presents the prototypes and their properties, and Figure 5 shows a nano-HIPE that is unstable under thermal conditions (a) and another that is unstable during freeze/thaw cycles (b).

**Table 4.** Physicochemical properties and nano-HIPE stability of polyglycerol esters containing several fatty acids grafted onto the same PG10.

| | **PG10-MCT** | **PG10-HPKO** | **PG10-HPO** | **PG10-Stearin** |
|---|---|---|---|---|
| Abbreviation | PG10MCT | PG10HPKO | PG10HPO | PG10C16C18 |
| Fatty acid composition | Triglycerides of capric and caprylic acids (C8 and C10) | Triglycerides with fatty acids from C8 to C18 with C12 in large majority | Triglycerides of palmitic and stearic acids (C16/C18) | Mixture of free palmitic and stearic acids (C16/C18) |
| HLB | 15.5 ± 0.5 | 13.0 ± 0.5 | 10.0 ± 0.5 | 11.0 ± 0.5 |
| Nano-HIPE stability 3 months at 40 °C | OK | OK | OK | OK |
| Nano-HIPE stability 1 month at 50 °C | Not OK | Not OK | OK | OK |
| Nano-HIPE stability after 3 freeze/thaw cycles | OK | OK | Not OK | Not OK |



(**a**) (**b**)

**Figure 5.** Photographs of unstable nano-HIPEs: (**a**) at elevated temperature; (**b**) during freeze/thaw cycling.

Regarding the HLB values, it can be observed that the longer the aliphatic chain of the fatty acids used, the lower the HLB value. This is due to the increased hydrophobic character of the surfactant, which reduces its affinity for water and consequently lowers its HLB. Conversely, shorter fatty acid chains lead to higher HLB values due to the decrease in the size of the hydrophobic part.

According to Table 4, PG10MCT and PG10HPKO made it possible to obtain nano-HIPEs that were stable during freeze/thaw cycles and at 40 °C but not at 50 °C. Conversely, PG10HPO and 10C16C18 prototypes produced a concentrated gel emulsions that were stable at 40 and 50 °C but not during freeze/thaw cycles. These observations suggest that short-chain fatty acids (<C16) contribute to freeze–thaw stability, whereas long-chain fatty acids (≥C16) enhance thermal stability at elevated temperatures.

The hypothesis proposed to explain why longer aliphatic chains yield nano-HIPEs with greater thermal stability than shorter chains relates to the melting behavior of the corresponding esters. In nano-HIPEs, the oil droplets are packed very closely due to the high internal phase volume, which inherently promotes coalescence. When nano-HIPEs formulated with PG10MCT or PG10HPKO are heated, the interfacial surfactants melt and become liquid, facilitating droplet coalescence. In contrast, PG10HPO and PG10C16C18, which contain long-chain fatty acids, do not melt at 40 °C or 50 °C, allowing the resulting nano-HIPEs to remain stable under these conditions.

The opposite trend was observed during freeze–thaw cycles. Short-chain and medium-chain esters (PG10MCT and PG10HPKO) form small crystals, whereas long-chain esters (PG10HPO and PG10C16C18) generate large crystals. These larger crystals behave like needles that can pierce the droplets upon freezing [36,38]. In addition, the water phase freezes and expands, increasing internal stress within the system. So, with long-chain esters, the interface between the droplets breaks down due to a lack of flexibility. The system needs flexibility with a low melting point for the surfactants to withstand freeze/thaw cycles.

Furthermore, the length of the surfactant's aliphatic chains also influences the rheological properties of the formulation, which in turn influences its stability. PG10 esters with long-chain fatty acids yield more viscous nano-HIPEs, resulting in reduced droplet mobility. For example, nano-HIPE made with PG10MCT have a viscosity of 15,040 cP while the nano-HIPE made with PG10HPO had a viscosity of 308,000 cP. The stabilization mechanism promoted by PG10 esters in nano-HIPEs is thus associated with steric hindrance between oil droplets within the gelled emulsion [11]. This steric hindrance limits surfactant mobility and consequently reduces destabilization phenomena such as coalescence or flocculation, thereby enhancing thermal stability.

Based on these results, we decided to synthesize polyglycerol esters containing a mixture of short/medium and long fatty acids grafted onto the same polyglycerol.

#### 3.1.4. Polyglycerol Esters with Mixture of Various Short/Medium and Long Chains FAs: PG10-Short and Long nFA

Three new prototypes were synthesized by using blends of short/medium-chain fatty acids (from MCT, HPKO, or myristic acid) and long-chain fatty acids (from stearin). Their characteristics and the resulting stability of the nano-HIPEs formulated with them are presented in Table 5 and a picture of the formulated nano-HIPE is shown in Figure 6.

**Table 5.** Physicochemical characteristics of polyglycerol-10 esters containing mixed long- and short-chain fatty acids and the resulting nano-HIPE stability.

| | **PG10-MCT-Stearin** | **PG10-HPKO-Stearin** | **PG10-C14-Stearin** |
|---|---|---|---|
| Abbreviation | MCT/S | HPKO/S | C14/S |
| Fatty acid composition | Stearin and caprylic/capric triglycerides (C8/C10) | Stearin and triglycerides from hydrogenated palm kernel oil (C12/C14) | Stearin and myristic acid (C14) |
| HLB | 12.0 ± 0.5 | 11.5 ± 0.5 | 11.5 ± 0.5 |
| Nano-HIPE stability 3 months at 40 °C | OK | OK | OK |
| Nano-HIPE stability 1 month at 50 °C | OK | OK | OK |
| Nano-HIPE stability after 3 freeze/thaw cycles | OK | OK | OK |

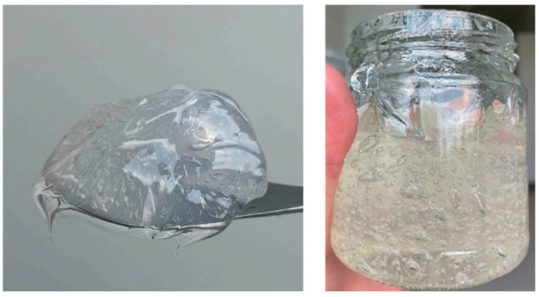


**Figure 6.** Stable nano-High Internal Phase Emulsion formulated with PG10-short and long nFA.

All prototypes synthesized using this strategy managed to make nano-HIPEs that met our stability criteria. The MCT/S, HPKO/S and C14/S were able to stabilize nano-HIPEs that remained stable for one month at 50 °C, three months at 40 °C and after three freeze/thaw cycles. These findings are consistent with previous hypotheses suggesting that short-chain fatty acids confer flexibility and stability during freeze/thaw cycles, whereas long-chain fatty acids confer thermal stability. This parameter seems to be one of the key factors for obtaining polyglycerol esters that are highly effective at stabilizing complex emulsions. Moreover, the HLB values also seem to play an important role in the effectiveness of the prototypes, as the three best-performing ones have an HLB of 11.5/12.0 $\pm$ 0.5.

The use of polyglycerol-10 esters with this combination of short/medium and long fatty acids also made it possible to reduce the concentration needed to stabilize this type of emulsion compared with conventional emulsifiers. Indeed, even with a very low concentration of PG10 ester (1.5 to 3%), it is possible to stabilize O/W emulsions when a minimum of 3–5% is recommended by sucrose ester suppliers, for example.

The droplet size of the nano-HIPE was measured directly on the degassed gel to avoid artefactual values arising from trapped air bubbles. Measurements were performed at 25 °C using photon correlation spectroscopy based on dynamic light scattering with a scattering angle of 90°. Dilution was avoided because it produces a turbid emulsion that cannot be analyzed with the instrument used. The resulting size distribution is shown in Figure 7. Since the software does not provide an autocorrelation function, this measurement should be considered indicative only. The nano-HIPE formulated with the MCT/S prototype exhibited an average droplet diameter of approximately 290 nm, which supports its classification as a "nano"-HIPE. This result was further supported by optical microscopy at $\times$400 magnification, where no droplets could be observed. The absence of visible structures at this magnification confirms that the droplets are submicron in size.

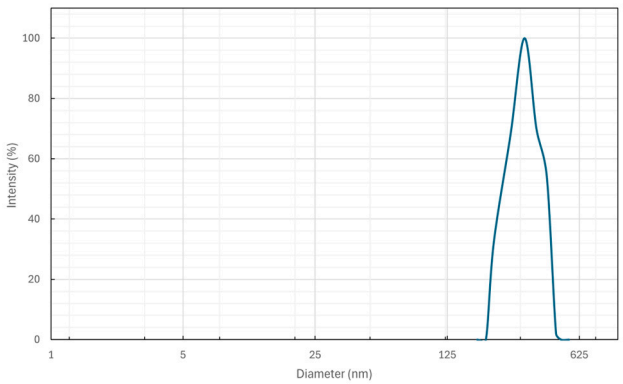



**Figure 7.** Droplet size distribution of a nano-HIPE formulated with MCT/S measured by DLS.

3.1.5. Presence of Partial Glycerides in the Functional Behavior of Polyglycerol-10 Esters

The three prototypes MCT/S, HPKO/S, and C14/S enable the formulation of stable nano-HIPEs using the formula described above (3 wt% of PG10 ester to be tested, 5 wt% water; 9 wt% glycerin and 83 wt% MCT. To assess their robustness, we evaluated their performance with organic phases other than MCT. Indeed, a surfactant is not economically viable if it performs adequately only in a single formulation. For this reason, the three prototypes were tested in nano-HIPEs formulated with various cosmetic oils as the oil phase. The results are presented in Table 6: a green checkmark indicates nano-HIPE that remained stable at room temperature, 40 °C, 50 °C and after three freeze/thaw cycles, whereas a red cross denotes a nano-HIPE that did not meet these stability criteria.

**Table 6.** Stability of nano-HIPEs formulated with various cosmetics oils and polyglycerol ester prototypes.

| Oily Phase (INCI Name) | MCT/S | HPKO/S | C14/S |
|---|---|---|---|
| Caprylic/Capric triglycerides | ✔ | ✔ | ✔ |
| Coco-caprylate/caprate | ✔ | ✔ | X |
| Octyldodecyl myristate | ✔ | ✔ | X |
| Isostearyl isostearate | ✔ | ✔ | ✔ |
| Hydrogenated polydecene | ✔ | ✔ | X |

X = No formation of stable nano-HIPE according to our criteria. ✔ = Formation of stable nano-HIPE according to our criteria.

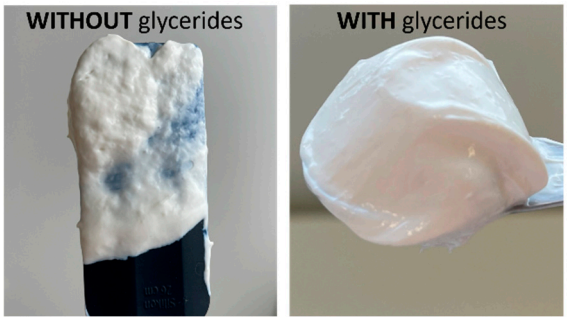
According to Table 6, the MCT/S and HPKO/S prototypes enabled the formulation of nano-HIPEs that meet our stability criteria with all the oils tested. In contrast, C14/S allows stable nano-HIPEs to be obtained with only two oils, caprylic/capric triglycerides and isostearyl isostearate. The only structural difference between these prototypes is that MCT/S and HPKO/S contain residual glycerides due to their transesterification-based synthesis, whereas C14/S does not. Indeed, MCT/S and HPKO/S were synthesized from polyglycerol, free fatty acids, and triglyceride oil, while C14/S contains only PG10 and free fatty acids. Based on this observation, we hypothesized that partial glycerides improve the stabilizing performance of polyglycerol esters acting as cosurfactant by making them more versatile.

To confirm this hypothesis, the HPKO/S prototype was tested in the formulation of sunscreen emulsions in comparison with another prototype containing exactly the same fatty acid composition but without residual glycerides (called FA/S). The sunscreen formula used was the one presented above, as it represents a challenge in terms of feasibility and stability. It is a direct emulsion containing a large amount of mineral UV filters to achieve high SPFs. The results obtained with the two different prototypes, with and without glycerides, are shown in Figure 8.

We can see in Figure 8 that the emulsion made with the prototype without glyceride was heterogeneous and unstable. In contrast, the emulsion made with the prototype containing partial glycerides was homogeneous and stable according to our criteria.

To ensure that this difference in effectiveness in stabilizing these complex emulsions was indeed due to the glycerides, a new prototype was synthesized in an attempt to recreate these glycerides. Specifically, polyglycerol, C8 to C18 fatty acids corresponding to the fatty acid composition of hydrogenated palm kernel oil, and glycerol were placed into the reactor to form partial glycerides by esterification. This prototype was then tested in the sunscreen emulsion and in nano-HIPE formulations with different oil phases: caprylic/capric triglycerides (MCT), octyldodecyl myristate (MOD), and coco-caprylate/caprate (Cetiol® C5).

The results are presented in Table 7 and compared to those of the prototypes HPKO/S and FA/S (the prototype without glycerides).




(**a**) (**b**)

**Figure 8.** O/W mineral sunscreen emulsions formulated with: (**a**) a PG10 ester without partial glycerides (FA/S); (**b**) a PG10 ester containing partial glycerides (HPKO/S).

**Table 7.** Formulation outcomes for polyglycerol esters prototypes without glycerides (FA/S), with oil-derived glycerides (HPKO/S) and with synthesized glycerides (Gly/FA/S).

| | **FA/S** | **Gly/FA/S** | **HPKO/S** |
|---|---|---|---|
| Presence/absence of glycerides | Without glycerides | With glycerides from synthesis | With glycerides from oil |
| HLB | 11.0 ± 0.5 | 11.5 ± 0.5 | 11.5 ± 0.5 |
| Mineral sun emulsion | Not OK even at RT | OK | OK |
| Nano-HIPE with MCT | OK | OK | OK |
| Nano-HIPE with MOD | NOK (cycle) | OK | OK |
| Nano-HIPE with Cetiol® C5 | NOK (cycle and heat) | OK | OK |

These results demonstrate that glycerides play a crucial role in the performance of polyglycerol esters. Indeed, Table 7 shows that it was only possible to obtain mineral O/W sunscreen emulsions that met our criteria with the prototypes containing glycerides (Gly /FA/S and HPKO/S). The FA/S prototype, which does not contain glycerides, did not produce a sunscreen emulsion that was stable at elevated temperatures or even at room temperature, and only the nano-HIPE formulated with MCT was stable according to our criteria. The glycerides in the Gly/FA/S and HPKO/S prototypes appear to act as co-surfactants, improving the performance of the surfactant and thus stabilizing emulsions that are demanding in terms of feasibility and stability [11].

According to the article by Fonseca, Santos et al. 2025 [11] glycerides (monoacylglycerides MAG and diacylglycerides DAGs) play two crucial roles in emulsion stabilization. They act as structuring agents in the oil phase by increasing its viscosity, thereby reducing the movement of oil droplets and preventing Oswald ripening. In addition, MAGs and DAGs act as co-surfactants by reducing the interfacial tension between droplets, resulting in improved emulsion stability [11,40]. A possible mechanism of action for the surfactants containing glycerides (MAGs, DAGs, and TAGs) and polyglycerol esters in their composition is shown in Figure 9. Here, polyglycerol esters with different aliphatic chain lengths and highly mobile monoglycerides are located at the oil/water interface. Diglycerides and triglycerides, which are larger and therefore less mobile, are located inside the oil droplets, thus structuring the fatty phase.

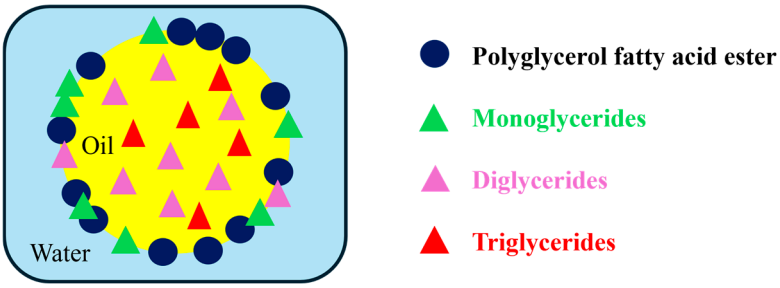



**Figure 9.** Schematic representation of the proposed stabilization mechanism for the HPKO/S and Gly/FA/S prototypes containing partial glycerides.

On the other hand, according to Smith, Bhaggan et al., 2011 [41] et Gordon, and Rahman 1991 [42], glycerides also play a role in fat crystallization. It has been proven that these minor components have an impact on the nucleation, crystal growth, morphology, and polymorphic stability of fat crystals. In our case, these partial glycerides therefore contribute to reducing the size of the crystals formed at the droplet interface, as explained above, thereby improving heat and cycle stability.

In conclusion, these observations support the previously formulated hypothesis that partial glycerides act as co-surfactants in these complex formulations, thereby making the use of the surfactant more versatile.

#### 3.1.6. New Generation Polyglycerol Esters: Use of Variety of Oils

The importance of combining short/medium-chain and long-chain fatty acids on the same polyglycerol, as well as the role of partial glycerides, has already been demonstrated. We therefore wanted to determine whether various oils could be used to synthesize these polyglycerol esters, or whether their composition was in fact more limited. Indeed, understanding whether different oil sources can be used helps to define the synthesis strategy.

To evaluate the versatility of these polyglycerol esters, three prototypes were synthesized. Specifically, three oils with similar fatty acid compositions but different origins were tested. The properties of these surfactants, as well as the stability of the nano-HIPEs formulated with them, are presented in Table 8. The prototype Cuphea/S contains oil extracted from the Cuphea plant, supplied by the USDA ARS National Center for Agricultural Utilization Research (Peoria, Illinois). The prototype HCO/S is composed of a hydrogenated coconut oil (coprah) which has a fatty acid composition was similar to that of hydrogenated palm kernel oil. And finally, the Hilucia/S prototype is synthesized using insect oil supplied by Innovafeed. This oil, derived from the black soldier fly and rich in lauric acid, represents a sustainable alternative to tropical oils, as its production generates very few $CO_2$ emissions and has no impact on deforestation. Currently, its animal origin makes it difficult to use in cosmetics formulations, but it was tested from a sustainable perspective.

The three PG10 esters shown in Table 8 produce nano-HIPEs that are stable for at least 3 months at 40 °C and 1 month at 50 °C. As seen previously for HPOK/S, their HLB values were around 11.5/12, confirming that this HLB appears to be optimal for the formulation of this type of emulsion.

These results highlight the possibility of using a wide variety of oils for the manufacture of PG10 esters capable of stabilizing complex emulsions. The reverse approach is also feasible: combining long-chain fatty acid oils with short-chain fatty acids. The key requirement is maintaining an appropriate short/medium-chain to long-chain ratio to achieve an HLB close to 11–12.

**Table 8.** Physicochemical properties and nano-HIPE stability of polyglycerol esters synthesized from different oil sources: Cuphea, Coconut and Insect oils.

| | **PG10-Cuphea-Stearin** | **PG10-HCO-Stearin** | **PG10-Hilucia$^{TM}$-Stearin** |
|---|---|---|---|
| Abbreviation | Cuphea/S | HCO/S | Hilucia/S |
| Fatty acid composition | From Cuphea oil | From coconut oil | From Hermetia Illucens (insect) oil |
| HLB | 12.0 ± 0.5 | 11.5 ± 0.5 | 11.5 ± 0.5 |
| Stability 3 months at 40 °C | OK | OK | OK |
| Stability 1 month at 50 °C | OK | OK | OK |
| 3 cycles stability | OK | OK | OK |

### *3.2. Effect of the Manufacturing Process on the Fatty Acid Composition of Polyglycerol Esters*

The effect of the synthesis process on the fatty acid composition of polyglycerol-10 esters was also investigated in this study because the trials revealed that this parameter is critical for achieving optimal surfactant performance. The manufacturing process is not straightforward, and the polyglycerol ester's performance depends entirely on it.

Indeed, syntheses involving esterification reactions are typically monitored by measuring the acid value (AV) [43]. This parameter indicates the amount of acid remaining in the medium and thus helps to determine the end of the esterification. However, during the synthesis of the polyglycerol esters described above, it was observed that the reaction was not actually complete even when all the acids had been consumed. In fact, it was noted that the reaction medium which was initially turbid (t), became clear (c) after a certain reaction time, well after the acid value had fallen below 1 mg KOH/g. This phenomenon is shown in Figure 10.

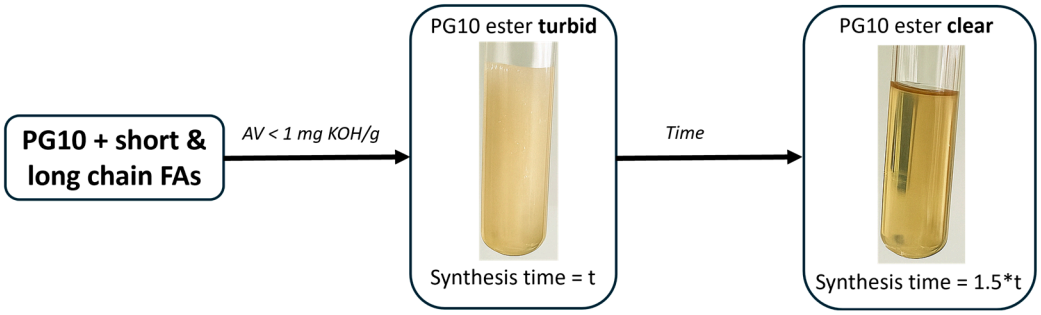



**Figure 10.** Flowchart process showing the change in the appearance of the reaction medium during the synthesis of polyglycerol-10 esters.

Therefore, experiments were conducted to assess the impact of achieving clarity on the efficiency of polyglycerol-10 esters. The prototypes were synthesized using different procedures: one in which the reaction was stopped when the acid value dropped below 1 mg KOH/g and the product was turbid (C8C10/S(t) and C8-18/S(t)), and another in which the reaction was stopped once the product became clear (C8C10/S(c) and C8-18/S(c)). The characteristics and the stability performance of the resulting prototypes are presented in Table 9.

In this study, prototypes C8C10/S(t) and C8C10/S(c) have exactly the same fatty acid composition and must be compared with each other. The same applies to prototypes C8-18/S(t) and C8-18/S(c), which have the same composition but one is turbid and the other is clear. The results obtained from these experiments highlight the importance of the clarity parameter in the synthesis of polyglycerol esters for use in nano-HIPEs.

**Table 9.** Physicochemical characteristics and nano-HIPE stability of polyglycerol esters synthesized with or without achieving reaction medium clarity.

| | PG10-C8/C10-Stearin (Turbid) | PG10-C8/C10-Stearin (Clear) | PG10-C8C18-Stearin (Turbid) | PG10-C8C18-Stearin (Clear) |
|---|---|---|---|---|
| Abbreviation | C8C10/S(t) | C8C10/S(c) | C8-18/S(t) | C8-18/S(c) |
| Fatty acid composition | Stearin and caprylic/capric fatty acids | | Stearin, caprylic, capric fatty acids, lauric, myristic, palmitic and stearic fatty acids | |
| HLB | 7.0 ± 0.5 | 12.0 ± 0.5 | 6.0 ± 0.5 | 11.0 ± 0.5 |
| Nano-HIPE stability with MCT | Not OK even at RT | OK | Not OK even at RT | OK |

Indeed, as shown in Table 9 although the prototypes C8C10/S(t) and C8C10/S(c) are composed of exactly the same raw materials in identical proportions, they exhibit markedly different characteristics. C8C10/S(t) has an HLB of 7.0, whereas C8C10/S(c) has an HLB of 12.0. A similar trend is observed between the prototypes C8-18/S(t) and C8-18/S(c), where the turbid prototype has an HLB of 6.0, while the clear prototype shows an HLB of 11.0. The clarity of the reaction medium appears to have a significant impact on the HLB, which almost doubles between the turbid and clear prototypes.

On the other hand, based on the results in Table 9, it can be observed that C8/C10/S(t) and C8-18/S(t) do not allow the formation of stable nano-HIPEs. These emulsions either do not form or are not stable, even at room temperature. In contrast, C8C10/S(c) and C8-18/S(c) enable the formulation of stable nano-HIPEs with MCT as the oil phase, not only at room temperature but also at 40 °C and 50 °C and at three freeze/thaw cycles.

Furthermore, the clear prototypes were homogeneous at the end of the synthesis, whereas the turbid ones underwent phase separation with unreacted polyglycerol-10 found in the lower phase. In fact, clarity is related to the solubility of polyglycerol-10 in the surfactant. When the reaction medium is turbid, it is because some of the free polyglycerol-10 is not soluble in the surfactant, indicating that the reaction equilibrium has not yet been reached. But, when the reaction medium becomes clear, it means that all of the free PG10 is soluble in the surfactant, and the reaction equilibrium has been reached. The hypothesis is that the transition from a turbid to a fully clear product is like a "critical solubility point" which could thus serve as a visual indicator confirming that the reaction has reached equilibrium and that the surfactant exhibits the expected properties (a high HLB, the correct amount of solubilized polyglycerol and good formulation performance).

This can be explained by the fact that, during synthesis, polyglycerol-10 is completely insoluble in fatty acids due to their strongly contrasting polarities, as previously discussed. Once a fatty acid is successfully grafted onto a PG10 molecule, the resulting ester becomes more soluble in the organic phase. This increased solubility then facilitates the successive grafting of additional aliphatic chains onto the same polyglycerol backbone. As a result, a large proportion of multi-esters, relatively hydrophobic, is initially formed. Once all the fatty acids are consumed, transesterification reactions occur, in which fatty acid chains from the multi-esters (which are soluble in both hydrophilic and lipophilic phases) are transferred to free PG10 molecules, preferentially forming monoesters. This explains why the HLB values of the clear prototypes are significantly higher than those of the turbid ones while the fatty acid composition remains the same: the clear prototypes likely contain more monoesters, which are more hydrophilic, whereas the turbid ones are richer in multi-esters. This also explains why the trouble prototypes have a lower HLB than the clear prototypes. Indeed, according to this hypothesis, the turbid prototypes contain a greater structural diversity of esters (tri-, tetra-, penta-esters, etc.) than the clear prototypes. Moreover,

polyglycerol-10 is not a linear polymer but exhibits branching and cyclic motifs within its structure. Consequently, the structural heterogeneity present in the turbid polyglycerol esters leads to a much more challenging self-assembly into micelles, as the molecules do not display a well-defined separation between hydrophilic and lipophilic domains. These molecules therefore tend to remain dispersed individually in the medium rather than forming aggregates. This results in a higher CMC, since a larger number of ester molecules is required in the medium before micellar organization can occur.

To support this hypothesis, comparative chromatographic analyses of the four prototypes were performed using UHPLC-CAD/MS. These analyses focus only on the major species present in the ingredient, as polyglycerol is a complex mixture of oligomers and several fatty acids are involved. Consequently, the analysis focuses solely on the species predominantly present in the surfactant, which means the esters formed with the predominant PG oligomers combined with the main fatty acids (67 species in total).

Thanks to these analyses, Table 10 demonstrates that the cloudy prototypes contain fewer monoesters than the clear prototypes. C8C10/S(t) is composed of 58.8% monoesters, while C8C10/S(c) contains 63.8% and C8-18/S(t) contains 57.5% monoesters compared to C8-18/S(c), which contains 65.2%. These observations support our hypothesis and must therefore contribute to the increase in the HLB observed for the clear prototypes.

**Table 10.** Ester type composition of prototypes C8C10/S(t), C8C10/S(c), C8-18/S(t) and C8-18/S(c).

| | **C8C10/S(t)** | **C8C10/S(c)** | **C8-18/S(t)** | **C8-18/S(c)** |
|---|---|---|---|---|
| HLB | 7.0 ± 0.5 | 12.0 ± 0.5 | 6.0 ± 0.5 | 11.0 ± 0.5 |
| Monoesters (%) | 58.8 | 63.8 | 57.5 | 65.2 |
| Diesters (%) | 41.2 | 36.2 | 42.5 | 34.5 |

The free polyglycerol solubilized in the clear prototypes may also play a role in this high HLB value. Indeed, the presence of non-esterified polyglycerol can modulate the interfacial structure of the esters present and thus modify their interfacial behavior by interacting physiochemically with them [44]. Free polyglycerol can associate with esters through hydrogen bonds or Van Der Waals interactions, or create hybrid micellar or lamellar assemblies that modify the solubility and distribution of components at the interface. It can also increase the solubility of esters in the aqueous phase, which can improve their adsorption at the interface and thus act as if their HLB were higher.

All observations indicate that the synthesis process significantly influences the relative composition of polyglycerol esters and so the emulsifying properties of the surfactant. The transition to clarity of the reaction mixture is a visual indicator that the reaction equilibrium has been reached, that all residual polyglycerol-10 has been solubilized, and that the final product will perform as expected.

## 4. Conclusions

It has been demonstrated that several parameters are decisive for the development of a polyglycerol-10 ester capable of stabilizing complex emulsions, such as high internal phase nano-emulsions or sunscreen emulsions with a high mineral filter content. The polyglycerol-10 ester must be composed of several different fatty acids grafted onto the same polyglycerol (reaction in one-pot). In addition, the fatty acids must be a mixture of short/medium-chain fatty acids (<C16) and long-chain fatty acids (≥C16). Furthermore, the presence of partial glycerides in the surfactant is required to achieve the expected performance in terms of stability and to obtain greater versatility in the use of the surfactant. Finally, the synthesis

process, with clarity as an indicator of the end of the reaction, proved to be a key parameter for obtaining a surfactant with optimized performance.

This study proposes a promising solution for formulating emulsions with high stability and feasibility requirements, using surfactants that are both environmentally friendly and easy to use.

Several avenues would merit further investigation to deepen the understanding of polyglycerol esters in complex formulations. A more detailed study of how the fatty acid composition of polyglycerol esters influences their performance in stabilizing mineral sunscreen formulations would be particularly valuable. In addition, examining the crystallinity of the various polyglycerol-10 esters synthesized could help clarify the mechanisms underlying their temperature-dependent instabilities. Finally, exploring the impact of the fatty-acid composition on other physicochemical properties, such as the critical micelle concentration, would provide further insight into the structure–function relationships governing these surfactants.

**Author Contributions:** Conceptualization, J.R., M.N. and J.-D.R.; Methodology, J.R., M.N. and J.-D.R.; Investigation, J.R., M.N. and N.R.; Writing—original draft preparation, J.R.; Formal analysis, J.R. and N.R.; Data curation, M.N. and J.-D.R.; Writing—review and editing, M.N. and J.-D.R.; Project administration M.N. and J.-D.R.; Supervision, M.N. and J.-D.R. All authors have read and agreed to the published version of the manuscript.

**Funding:** This research received no external funding.

**Institutional Review Board Statement:** Not applicable.

**Informed Consent Statement:** Not applicable.

**Data Availability Statement:** The data presented in this study are available on request from the corresponding author.

**Conflicts of Interest:** The authors declare no conflicts of interest.

## References

1. Sasounian, R.; Martinez, R.M.; Lopes, A.M.; Giarolla, J.; Rosado, C.; Magalhães, W.V.; Velasco, M.V.R.; Baby, A.R. Innovative Approaches to an Eco-Friendly Cosmetic Industry: A Review of Sustainable Ingredients. *Clean Technol.* **2024**, *6*, 176–198. [CrossRef]
2. Spaulding, A.; Baki, G. Sustainable cosmetic ingredient alternatives to replace conventional ingredients: Case studies in moisturizers and lipsticks. *Int. J. Cosmet. Sci.* **2026**, *48*, 83–96. [CrossRef] [PubMed]
3. Goyal, N.; Jerold, F. Biocosmetics: Technological advances and future outlook. *Environ. Sci. Pollut. Res. Int.* **2023**, *30*, 25148–25169. [CrossRef] [PubMed]
4. Alviri, H.; Lynes, J.; Habib, K. Beyond green chemistry: A comprehensive review of how sustainability has been integrated into cosmetic research. *Glob. Sustain.* **2025**, *8*, e16. [CrossRef]
5. Pasternak, G.; Askitosari, T.D.; Rosenbaum, M.A. Biosurfactants and Synthetic Surfactants in Bioelectrochemical Systems: A Mini-Review. *Front. Microbiol.* **2020**, *11*, 358. [CrossRef]
6. Ruckenstein, E.; Ebert, G.; Platz, G. Phase behavior and stability of concentrated emulsions. *J. Colloid Interface Sci.* **1989**, *133*, 432–441. [CrossRef]
7. Hu, X.; Binks, B.P.; Cui, Z. High internal phase emulsions stabilized by adsorbed sucrose stearate molecules and dispersed vesicles. *Food Hydrocoll.* **2021**, *121*, 107002. [CrossRef]
8. Sagitani, H.; Hattori, T.; Nabeta, K.; Nagai, M. Formation of O/W emulsion having fine and uniform droplets by the surfactant D phase emulsification method. *Nippon Kagaku Kaishi* **1983**, *10*, 1399–1404. [CrossRef]
9. Chen, X.-H.; Tang, C.-H. Transparent high internal phase emulsion gels stabilized solely by proteins. *Colloids Surf. A Physicochem. Eng. Asp.* **2021**, *608*, 125596. [CrossRef]
10. Kim, H.-J.; Jeong, N.-H.; Kim, H.-S.; Lee, Y.; Nam, K.-D. Preparation and properties of D phase emulsion by silicone oil. *J. Korean Ind. Eng. Chem.* **1999**, *10*, 809–813.
11. Fonseca, L.R.; Santos, M.A.S.; Silva, T.J.; Santos, T.P.; Cunha, R.L. High internal phase water-in-oil emulsions: Trends and challenges on production and stabilization. *J. Am. Oil Chem. Soc.* **2025**, *102*, 509–520. [CrossRef]

12. Chen, Q.; Tai, X.; Li, J.; Li, C.; Guo, L. High internal phase emulsions solely stabilized by natural oil-based nonionic surfactants as tea tree oil transporter. *Colloids Surf. A Physicochem. Eng. Asp.* **2021**, *616*, 126320. [CrossRef]
13. Murakami, A.; Fukada, K.; Yamano, Y.; Gohtani, S. Effects of Sucrose on Emulsification of Triglyceride by Polyglycerin Fatty Acid Ester. *J. Oleo Sci.* **2005**, *54*, 335–340. [CrossRef]
14. Sagitani, H. Formation of Fine Emulsions by Surface Chemical Methods. *J. Jpn. Oil Chem. Soc.* **1986**, *35*, 198–202. [CrossRef]
15. Zhao, R.; Chang, Z.; Jin, Q.; Li, W.; Dong, B.; Miao, X. Heterogeneous base catalytic transesterification synthesis of sucrose ester and parallel reaction control. *Int. J. Food Sci. Technol.* **2014**, *49*, 854–860. [CrossRef]
16. Hill, K.; Rhode, O. Sugar-based surfactants for consumer products and technical applications. *Fett/Lipid* **1999**, *101*, 25–33. [CrossRef]
17. Marcin, S.; Aleksander, A. Acute toxicity assessment of nine organic UV filters using a set of biotests. *Toxicol. Res.* **2023**, *39*, 649–667. [CrossRef]
18. Sun, Y.-H.; Wu, H.-Y.; Xie, F.-Q.; Ma, J.-R.; Tang, Q.-L.; Chen, Y.-F.; Li, H.; Liu, Y.-S.; Ying, G.-G. Environmental contamination and risks of organic UV filters: Source, discharge, analytical methods and implications for ecological and human health. *Sci. Total Environ.* **2024**, *955*, 176930. [CrossRef] [PubMed]
19. Schneider, S.L.; Lim, H.W. A review of inorganic UV filters zinc oxide and titanium dioxide. *Photodermatol. Photoimmunol. Photomed.* **2019**, *35*, 442–446. [CrossRef]
20. Lafranconi, M.; Anderson, J.; Budinsky, R.; Corey, L.; Forsberg, N.; Klapacz, J.; LeBaron, M.J. An integrated assessment of the 1,4-dioxane cancer mode of action and threshold response in rodents. *Regul. Toxicol. Pharmacol.* **2023**, *142*, 105428. [CrossRef]
21. Kandeel, E.M. Synthesis and Performance of Glycerol Ester-Based Nonionic Surfactants. *J. Dispers. Sci. Technol.* **2012**, *33*, 949–954. [CrossRef]
22. Ai, S.; Ishitobi, M. Effects of the number of fatty acid residues on the phase behaviors of decaglycerol fatty acid esters. *J. Colloid Interface Sci.* **2006**, *296*, 685–689. [CrossRef] [PubMed]
23. Sakamoto, M.; Ohba, A.; Kuriyama, J.; Maruo, K.; Ueno, S.; Sato, K. Influences of fatty acid moiety and esterification of polyglycerol fatty acid esters on the crystallization of palm mid fraction in oil-in-water emulsion. *Colloids Surf. B Biointerfaces* **2004**, *37*, 27–33. [CrossRef] [PubMed]
24. Sakamoto, M.; Fukunaga, K.; Kuriyama, J.; Sato, K. Retardation Effects of Polyglycerol Fatty Acid Esters on the Crystallization of n-Hexadecane. *J. Oleo Sci.* **2005**, *54*, 211–216. [CrossRef]
25. Zhang, M.; Zhang, G. Recent Advances in the Properties and Applications of Polyglycerol Fatty Acid Esters. *Polymers* **2025**, *17*, 879. [CrossRef]
26. Nollet, M.; Boulghobra, H.; Calligaro, E.; Rodier, J.-D. An efficient method to determine the Hydrophile-Lipophile Balance of surfactants using the phase inversion temperature deviation of Ci Ej /n-octane/water emulsions. *Int. J. Cosmet. Sci.* **2019**, *41*, 99–108. [CrossRef]
27. Amari, J.F.A.A.; Sangiorgio, S.; Pargoletti, E.; Rabuffetti, M.; Zaccheria, F.; Usuelli, F.; Quaranta, V.; Speranza, G.; Cappelletti, G. Chemically vs Enzymatically Synthesized Polyglycerol-Based Esters: A Comparison between Their Surfactancy. *ACS Omega* **2023**, *8*, 26405–26413. [CrossRef] [PubMed]
28. Griffin, W.C. Classification of Surface-Active Agents by "HLB". *J. Soc. Cosmet. Chem.* **1949**, *1*, 311–326. Available online: https://www.scirp.org/reference/referencespapers?referenceid=1610208 (accessed on 24 March 2026).
29. Lemahieu, G.; Ontiveros, J.F.; Molinier, V.; Aubry, J.-M. Using the dynamic Phase Inversion Temperature (PIT) as a fast and effective method to track optimum formulation for Enhanced Oil Recovery. *J. Colloid Interface Sci.* **2019**, *557*, 746–756. [CrossRef]
30. Toda, A. DSC techniques and phase transition kinetics. *Thermochim. Acta* **2026**, *761*, 180313. [CrossRef]
31. Sagitani, H.; Hirai, Y.; Nabeta, K.; Nagai, M. Effect of Types Polyols on Surfactant Phase Emulsification. *J. Jpn. Oil Chem. Soc.* **1986**, *35*, 102–107. [CrossRef]
32. Zhang, W.; Qin, Y.; Gao, Z.; Ou, W.; Zhu, H.; Zhang, Q. Phase behavior and stability of nano-emulsions prepared by D phase emulsification method. *J. Mol. Liq.* **2019**, *285*, 424–429. [CrossRef]
33. Kunieda, H.; Tanimoto, M.; Shigeta, K.; Rodriguez, C. Highly concentrated cubic-phase emulsions: Basic study on D-phase Emulsification using isotropic gels. *J. Oleo Sci.* **2001**, *50*, 633–639. [CrossRef]
34. Kirkbride, L.; Humphries, L.; Kozielska, P.; Curtis, H. Designing a Suitable Stability Protocol in the Face of a Changing Retail Landscape. *Cosmetics* **2021**, *8*, 64. [CrossRef]
35. Yann, G. D-Phase Del Technology, 2022. Available online: https://www.cosmetikwatch.com/fr/actualites/le-gel-d-phase-une-formulation-innovante-et-naturelle-pour-l-industrie-cosmetique-79.htm (accessed on 15 April 2025).
36. Springinsfeld, F. Mécanismes de Gélification et Comportement Rhéologique D'émulsions D'alcanes Partiellement Cristallisés. Ph.D. Thesis, Université Pierre et Marie Curie, Paris VI, Paris, France, 2009.
37. Relkin, P.; Sourdet, S.; Smith, A.K.; Goff, H.D.; Cuvelier, G. Effects of whey protein aggregation on fat globule microstructure in whipped-frozen emulsions. *Food Hydrocoll.* **2006**, *20*, 1050–1056. [CrossRef]

38. Thivilliers, F. *Gels D'émulsions à Base D'huiles Cristallisables: Mécanismes de Formation et Propriétés Rhéologiques; Matière Condensée [cond-mat]; NNT:.tel-00264651*; Université Sciences et Technologies—Bordeaux I: Talence, France, 2007. (In French)
39. Bunjes, H.; Koch, M.H.J.; Westesen, K. Effects of surfactants on the crystallization and polymorphism of lipid nanoparticles. In *Molecular Organisation on Interfaces*; Lagaly, G., Ed.; Springer: Berlin/Heidelberg, Germany, 2006; pp. 7–10. ISBN 978-3-540-43637-9.
40. Valoppi, F.; Calligaris, S.; Barba, L.; Šegatin, N.; Poklar Ulrih, N.; Nicoli, M.C. Influence of oil type on formation, structure, thermal, and physical properties of monoglyceride-based organogel. *Eur. J. Lipid Sci. Technol.* **2017**, *119*, 1500549. [CrossRef]
41. Smith, K.W.; Bhaggan, K.; Talbot, G.; van Malssen, K.F. Crystallization of Fats: Influence of Minor Components and Additives. *J. Am. Oil Chem. Soc.* **2011**, *88*, 1085–1101. [CrossRef]
42. Gordon, M.H.; Rahman, I.A. Effects of minor components on the crystallization of coconut oil. *J. Am. Oil Chem. Soc.* **1991**, *68*, 577–579. [CrossRef]
43. Vitolo, M.; Neves Rodrigues Ract, J.; Anunciação Braga Guebara, S. Feasibility on the Use of Acid Value for Evidencing the Esterification of Glycerol with Caprylic Acid Catalyzed by Lipase. *Athens J. Sci.* **2017**, *4*, 21–36. [CrossRef]
44. Shikhaliev, K.S.; Stolpovskaya, N.V.; Krysin, M.Y.; Zorina, A.V.; Lyapun, D.V.; Zubkov, F.I.; Yankina, K.Y. Production and Emulsifying Effect of Polyglycerol and Fatty Acid Esters with Varying Degrees of Esterification. *J. Am. Oil Chem. Soc.* **2016**, *93*, 1429–1440. [CrossRef]


**Disclaimer/Publisher's Note:** The statements, opinions and data contained in all publications are solely those of the individual author(s) and contributor(s) and not of MDPI and/or the editor(s). MDPI and/or the editor(s) disclaim responsibility for any injury to people or property resulting from any ideas, methods, instructions or products referred to in the content.